Impact of Thermal Radiation by Electron Beam on Inner Thermal State of Traveling Wave Tube

Jin Zhang, *Member, IEEE*, Changsheng Shen, *Member, IEEE*, Jinyan Wang, Yanmei Wang, Jinjun Feng, *Senior Member, IEEE*, Litao Sun, *Member, IEEE*, and Xiaohan Sun, *Member, IEEE*

***Abstract*—In this article, the impact of thermal radiation by the electron beam on the inner thermal state of a traveling wave tube (TWT) under operation is explored. A theoretical model for analyzing heat transfer by thermal radiation from the cylindrical electron beam is derived, in which the electron beam is treated as an equivalent dynamic circular disk with gray-body radiation from its side surface. By using the cathode temperature and the compression ratio of the electron beam in a TWT, the temperature of the equivalent disk is calculated. By considering the Bremsstrahlung radiation and the cyclotron radiation, the power radiated from the electron beam is derived, and the emissivities of the gray-body radiation from the equivalent disk are calculated. Using the parameters of a wideband TWT, we obtain the heat transfer via thermal radiation from the electron beam and conduct thermal analysis by simulation with and without considering thermal radiation from the electron beam, respectively. The result at 11 GHz shows that the temperature rise on the inner surface of the helix tape due to thermal radiation from the electron beam is 0.67 °C and 0.49 °C at the beginning/ending point of the helix, respectively. In the working frequency band, the temperature rise at the beginning point of the helix ranges from 0.65 °C to 0.72 °C, while that at the ending point ranges from 0.46 °C to 0.52 °C.**

***Index Terms*—Electron beam, helix traveling wave tube (TWT), thermal radiation, thermal state.**

I. Introduction

IT HAS been proven that the inner thermal state of the helix traveling wave tube (TWT), an important type of vacuum electron device (VED), can significantly impact its working performance, including changes in its high-frequency characteristics [1], output power [2], and its reliability [3]. Moreover, our recent study has shown that thermal deformation of the slow wave structure (SWS) is one of the contributing factors for backward wave oscillation (BWO) [4]. Consequently, the inner thermal state of the TWT is of great interest to the vacuum electronics community, and it has been analyzed by various methods [5]. In the existing thermal analyses, thermal sources, including ohmic loss and electron collision loss [6], [7], have been considered. However, another factor, the thermal radiation from the electron beam, has thus far not been examined, to our knowledge.

Received 29 May 2025; revised 12 October 2025; accepted 24 November 2025. Date of publication 12 January 2026; date of current version 13 February 2026. This work was supported in part by the National Key Scientific Research Program of China under Grant 2013CB933600 and in part by the National Key Laboratory Foundation on Vacuum Electronics of China under Grant 1510147. The review of this article was arranged by Senior Editor C. A. Ekdahl. *(Jin Zhang and Changsheng Shen are co-first authors.) (Corresponding author: Xiaohan Sun.)*

Jin Zhang, Changsheng Shen, Jinyan Wang, Litao Sun, and Xiaohan Sun are with the Research Center for Electronic Device and System Reliability, School of Electronic Science and Engineering, Southeast University, Nanjing 210096, China (e-mail: xhsun@seu.edu.cn).

Yanmei Wang and Jinjun Feng are with Beijing Vacuum Electronics Research Institute, Beijing 100016, China.

Color versions of one or more figures in this article are available at https://doi.org/10.1109/TPS.2025.3645111.

Digital Object Identifier 10.1109/TPS.2025.3645111

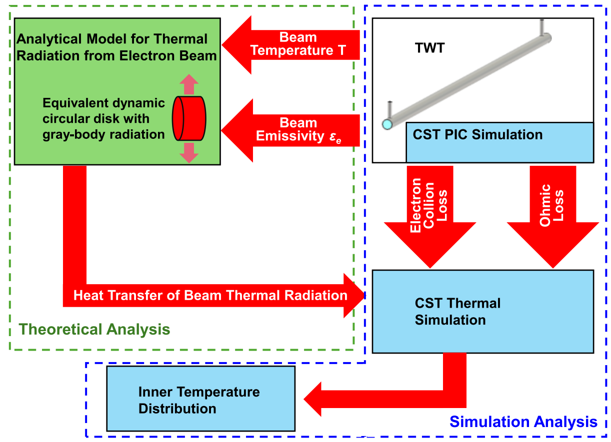

Fig. 1. Method for analyzing the impact of thermal radiation from the electron beam on the inner state of TWT.

Thermal radiation is a fundamental phenomenon for all objects, and the Stefan–Boltzmann law states that the radiated power is proportional to the fourth power of the absolute temperature [8], indicating that radiation from hot bodies may be significant. The temperature of the electron beam in a VED is usually of the order of 10^4 K [9], suggesting that the thermal radiation from the electron beam could be significant in contributing to the temperature rise inside the VED. Therefore, it would be desirable to analyze the thermal radiation from the electron beam so that all factors contributing to the inner thermal state of the VED are incorporated. Incorporating the effects of beam thermal radiation will also help to enhance the simulation accuracy of commercial simulation codes such as CST Studio Suite, which currently can only consider thermal losses of electron collision and ohmic losses in particle-in-cell (PIC) simulation.

In previous studies on the thermal properties of an electron beam, the temperature of an electron beam is represented by its random transverse thermal velocities [10], and can be calculated by using the cathode temperature and the beam compression ratio [11]. It has been measured experimentally [12], and its effect on beam defocusing has been analyzed [13], [14]. However, as far as we know, there is no existing method to analyze the thermal radiation from an electron beam and its impact on the inner temperature of the TWT.

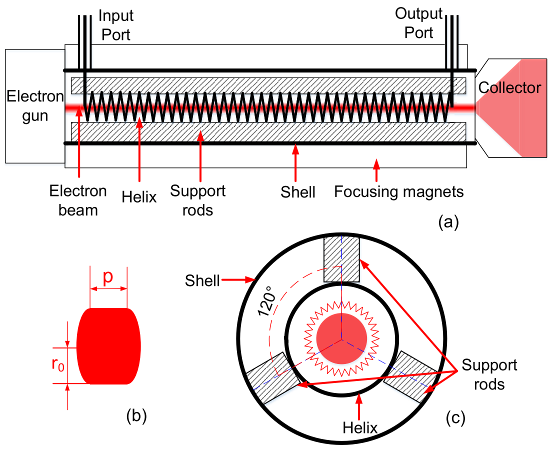

Fig. 2. Thermal radiation of electron beam in the helix TWT. (a) Schematic of the electron beam in the helix TWT. (b) Equivalent dynamic circular disk. (c) Model for analyzing thermal radiation from electron beam.

In this article, we propose a method for analyzing the thermal radiation from the electron beam and explore its impact on the inner thermal state of the TWT, as shown in Fig. 1. First, by treating the cylindrical electron beam as an equivalent dynamic circular disk with gray-body radiation from its side surface, a theoretical model is derived for analyzing the heat transfer by thermal radiation. Then, the thermal parameters of the electron beam, including the temperature and emissivity, are calculated theoretically. Finally, using the parameters of an actual wideband helix TWT, we calculate the radiation emissivity and power from the cylindrical electron beam, and analyze its impact on the inner thermal state of an operating TWT by simulation.

II. Model for Analyzing Thermal Radiation of Electron Beam

The operation of a TWT is based on the interaction between the electron beam and the traveling electromagnetic wave, thus amplifying the input signal to a much higher level. The cylindrical beam (or pencil beam) is the most widely used beam in the TWT, so we use the helix TWT to analyze the thermal irradiation of the cylindrical electron beam.

Fig. 2 shows the thermal radiation from the electron beam in the helix TWT. When the helix TWT is working, the electron gun produces the electron beam, which travels through the interaction space confined by the helix SWS and then is collected by the collector, as shown in Fig. 2(a). In this early stage study, we assume a uniform axial magnetic field for simplicity, and the theoretical treatment of thermal radiation is formulated accordingly. When the electron beam is in the interaction space, it can radiate heat to the helix, the support rods, and the tube shell. Considering that the electron beam has a small diameter and a relatively large length, it can be treated as a slender (thin) cylinder. From this, we may approximate the thermal radiation as occurring only on its side surface. To analyze the thermal radiation from the electron beam, we analyze a short segment of the electron beam, i.e., over the length of the helix pitch p, which is equivalent to a dynamic circular disk [15], with radius and thickness r_0 and p, respectively, as shown in Fig. 2(b). The disk temperature is assumed to be uniform due to its small size. It is also assumed that the disk is located at a fixed position where the incoming and outgoing electrons are in dynamic equilibrium, and the temperature of the disk is constant over time as the TWT is in a stable working condition. The disk is surrounded by the helix, three support rods spaced circularly (each pair is 120° apart), and the tube shell, as shown in Fig. 2(c). The radiation from the electron beam to the support rods/helix/shell is approximated as gray-body radiation such that the electron beam surface can be characterized by a temperature and an equivalent emissivity [16]. The gray-body radiation is a realistic model of the thermal radiation from a surface that absorbs and emits a constant fraction of the blackbody radiation. The emissivity of a gray-body ε is constant with wavelength, but $0 < \varepsilon < 1$, while $\varepsilon = 1$ for the blackbody. We also assume that the surface of the electron beam is a diffuse emission surface.

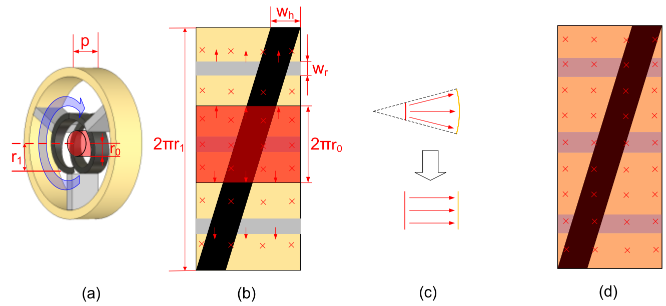

Fig. 3. Helix SWS in the TWT. (a) Normal structure. (b) Unfolding diagram in reference to the cylindrical surface of helix. (c) Extension of the surface of the electron beam. (d) Unfolded SWS, orange color denoting extended beam surface.

To obtain the net heat transfer between different surfaces, the view factors should be determined. The SWS is unfolded, as shown in Fig. 3, to allow calculation of the view factors. The normal SWS structure shown in Fig. 3(a) is unfolded, as illustrated in Fig. 3(b). The electron beam radius is r_0, so its unfolded area is given by $A_e = 2\pi r_0 p$; the helix radius is r_1, and its width is w_h, so its unfolded area is given by $A_h = 2\pi r_1 w_h$. Assuming that the thickness of the helix wire is negligible, the support rod width is w_r, so the unfolded area is given by $A_r = 3w_r(p-w_h)$; the inner radius of the tube shell is r_2, so the unfolded area is given by $A_s = 2\pi r_2 p$. Nonuniformity of the radiation from the electron beam toward the helix, the support rods, and the tube shell occurs in Fig. 3(b) due to the unfolding process. Therefore, the unfolded beam is further extended, as shown in Fig. 3(c), to ensure the uniformity of the radiation, and consequently, the ultimate unfolded SWS is obtained, as shown in Fig. 3(d). The view factors can be calculated using the formulas in [17]. Neglecting the thickness of the helix wire, the view factor between the electron beam and the helix can be obtained as follows:

$$F_{e-h} = \frac{w_h}{p}. \tag{1}$$

Similarly, neglecting the radiation on the side surface of the support rods, the view factor between the electron beam and the support rods is as follows:

$$F_{e-r} = \frac{3\,(p-w_h)\arctan\frac{w_r}{2r_1}}{\pi p}. \tag{2}$$

Since the heat generated by the electron beam radiation is absorbed by the helix, the support rods, and the tube shell, the view factor between the electron beam and the tube shell is

$$F_{e-s} = 1 - \frac{w_h}{p} - \frac{3\,(p - w_h)\arctan\frac{w_r}{2r_1}}{\pi p}. \quad (3)$$

Using the circuit analogy method in [14], we obtain the net heat transfer from the surface of the electron beam Q_{net}

$$Q_{\text{net}} = \frac{e_{b1} - B_1}{\frac{1-\varepsilon_{ec}}{\varepsilon_{ec}A_e}} = \frac{B_1 - B_2}{\frac{1}{A_e F_{e-h}}} + \frac{B_1 - B_3}{\frac{1}{A_e F_{e-r}}} + \frac{B_1 - B_4}{\frac{1}{A_e F_{e-s}}} \quad (4)$$

where e_{b1} is the radiosity (total flux of radiative energy away from a surface [16]) of a blackbody with the same temperature as the electron beam; B_1–B_4 are the radiosities from the electron beam, the helix, the support rods, and the tube shell, respectively; and ε_{ec} is the emissivity of the cylindrical electron beam. The first, second, and third terms on the right-hand side of (4) represent the net heat transfer from the electron beam to the helix, support rods, and shell, respectively. Considering that the temperature of the helix, support rods, and the shell is several hundred Kelvin [18], which is much lower than that of the electron beam, we neglect the heat transfer due to radiation among the helix, support rods, and the shell.

III. Temperature and Emissivity of Electron Beam

To analyze the thermal radiation from the electron beam using the model proposed in Section II, the temperature and the emissivity of the equivalent dynamic circular disk must be determined to calculate the radiosities B_1–B_4.

A. Temperature of Electron Beam

The microscopic measure of the temperature of a macroscopic object is the random thermal motion of the particles. The temperature of the electron beam can be expressed with the root-mean-squared velocity of the electrons [19]

$$v_{\text{rms}} = \sqrt{\frac{3k_B T_e}{m}} \quad (5)$$

where k_B is Boltzmann's constant, T_e is the temperature of the electron beam, and m is the electron mass. The temperature of the electron beam can be calculated by using the cathode temperature and the compression ratio [10], [11] as follows:

$$T_e = \frac{A_c}{A_b} T_c \quad (6)$$

where A_c is the cathode area, A_b is the cross-sectional area of the electron beam at the point where the temperature is measured, and T_c is the cathode temperature. In the above analysis, the temperature variation across the cross-sectional area of the electron beam is neglected.

B. Emissivity of Electron Beam

The electron beam confined by a magnetic field, usually known as pure electron plasma [20], is a type of nonneutral plasma [21]. The mechanism of thermal radiation from a conventional plasma includes Bremsstrahlung, recombination radiation, excitation radiation, and cyclotron radiation in magnetized plasmas [22]. However, there is no recombination radiation and excitation radiation in a pure electron plasma, so only the Bremsstrahlung and the cyclotron radiation need to be considered to calculate the emissivity of the equivalent dynamic disk.

1) Power by Bremsstrahlung Radiation: We use the equation in [23] to calculate the power by Bremsstrahlung radiation per unit volume per unit wavelength, which is expressed with Gaussian units

$$\frac{dP_B}{d\omega} = \frac{16n^2e^6}{15\text{m}^2c^5} v_{\text{rms}} \left(2\ln\frac{2v_{\text{rms}}}{\omega b_{\min}} + \frac{10}{3}\right) \quad (7)$$

where P_B is the radiated power by Bremsstrahlung per unit volume. ω is the angular frequency. n is the number density of the electrons. e is the unit charge. c is the speed of light. $b_{\min}$ is the minimum impact parameter, which satisfies the small-angle approximation for a pair of electrons on average, and it could be taken as the typical 90° deflection impact parameter ρ_{90° considering the slow logarithmic nature of the divergence [23]. According to [23], (7) applies in the range from $3\omega_p$ to ω_{90°

$$\omega_p = \sqrt{\frac{ne^2}{\varepsilon_0 m}} \quad (8)$$

where ω_p is the electron plasma frequency.

A reduction factor F must be added to the expression for the electron beam in the TWT [11], so (8) should be rewritten as

$$\omega_q = F\sqrt{\frac{ne^2}{\varepsilon_0 m}} \quad (9)$$

where ω_q is the reduced electron plasma frequency. The reduction factor F is determined by the structure parameters of the SWS in the TWT.

The ω_{90° is defined as

$$\omega_{90^\circ} = \frac{v_{\text{rms}}}{\rho_{90^\circ}}. \quad (10)$$

Considering that: 1) the radiation in the frequency band below $3\omega_p$ does not lie in the classical thermal radiation band [5]; and 2) the radiation over ω_{90° is negligibly slight [23], the radiation outside the frequency range is not considered.

We rewrite the expression in (7) in SI units, and transform the angular frequency into frequency; we obtain the Bremsstrahlung power per unit volume per unit frequency

$$P_f = \frac{n^2e^6 v_{\text{rms}}}{15\pi^2\text{m}^2c^5\varepsilon_0^3}\left(\ln\frac{v_{\text{rms}}}{\pi f b_{\min}} + \frac{5}{3}\right) \quad (11)$$

where P_f is the radiated power per unit volume per unit frequency and f is the frequency. Equation (11) applies in the frequency band from $3f_p$ to f_{90°, in which $f_p = \omega_p/2\pi$ and $f_{90^\circ} = \omega_{90^\circ/2^\circ}\pi$.

Integrating P_f from $3f_p$ to f_{90° (considering $f_{90^\circ} \gg 3f_p$), we obtain the power per unit volume by Bremsstrahlung

$$P_B = \int_{3f_p}^{f_{90^\circ}} P_f \,\text{d}f = 2\left(\frac{3\ln 2}{5} + 1\right)\frac{n^2e^4k_B^2T_e^2}{\pi^2m^3c^5\varepsilon_0^2}. \quad (12)$$

TABLE I
PARAMETERS OF ELECTRON BEAM AND SWS IN THE HELIX TWT

Parameter	Unit	Value
Electron density (n)	mm^{-3}	6.724×10^{13}
Cathode temperature	K	1423
Cathode area	mm^2	12.847
Magnetic flux density	Gauss	3100
Electron beam radius (r_0)	mm	0.42
Helix radius (r_1)	mm	1
Helix width (w_h)	mm	0.6
Helix pitch (p)	mm	1.1
Support rod width (w_r)	mm	0.3

2) Power by Cyclotron Radiation: In addition to Bremsstrahlung, thermal radiation from pure electron plasma occurs in the form of cyclotron radiation due to the transverse velocity of the electrons in the magnetic field [24]. Using the cyclotron radiation cooling theory in [24], we obtain the radiation power of the electron beam (in c.g.s.)

$$P_C = \frac{2ne^2\omega_c^2 v_{\perp,\mathrm{rms}}^2}{3c^3} \tag{13}$$

where P_C is the radiation power per unit volume; $v_{\perp,\mathrm{rms}}$ is the root mean square of the transverse velocity in the electron beam; and ω_c is the cyclotron frequency, which is given in [24] by the following expression:

$$\omega_c = \frac{eB_0}{mc} \tag{14}$$

where B_0 is the longitudinal magnetic flux density. Substituting (14) into (13) and expressing the result in SI units, we obtain the following equation:

$$P_C = \frac{ne^4 B_0^2 v_{\perp,\mathrm{rms}}^2}{6\pi \mathrm{m}^2 \varepsilon_0 c^3}. \tag{15}$$

3) Emissivity Calculation: For the equivalent circular disk of an electron beam mentioned previously in Section II, we have the following equation:

$$(P_B + P_C)\cdot \pi r_0^2 p = \varepsilon_{ec}\sigma T_e^4 \cdot 2\pi r_0 p \tag{16}$$

where σ is Stefan–Boltzmann's constant. Substituting (12) and (15) into (16), we obtain ε_{ec} as follows:

$$\varepsilon_{ec} = \frac{r_0 ne^4}{\pi\sigma T_e^4 \mathrm{m}^2\varepsilon_0 c^3}\left[\frac{B_0^2 v_{\perp,\mathrm{rms}}^2}{12} + \left(\frac{3\ln 2}{5}+1\right)\frac{nk_B^2T_e^2}{\pi mc^2\varepsilon_0}\right]. \tag{17}$$

IV. CALCULATION RESULTS

In this section, the model previously mentioned in Section II is analyzed based on the parameters of an actual wideband helix TWT, which are shown in Table I.

A. Heat Transfer of Thermal Radiation

By using (6), the electron beam temperature T_e is calculated to be 32 988 K. The transverse velocities of the electrons are composed of two parts: the transverse component of the gyrating motion in the electron beam and the transverse component of the random thermal velocities. The transverse root-mean-squared speed of the gyrating motion in the electron beam is simulated to be 1.1×10^7 m/s with CST, and the transverse root-mean-squared speed of random thermal motion at 32 988 K is calculated to be 1.23×10^6 m/s, whose square is negligible compared to that of the gyrating motion. Therefore, the transverse root-mean-squared speed of the electrons is considered to be 1.1×10^7 m/s.

By using (17), the emissivity of the electron beam ε_{ec} is calculated to be 4.34×10^{-10}. Based on our experience, the temperature of the SWS parts (helix, support rods, and tube shell) can be no more than 300 °C–400 °C (600–700 K) [18], which is much less than the electron beam temperature (32 988 K). The term T^4 of the SWS parts is approximately six orders of magnitude lower, so we neglect the radiosity from the helix, support rods, and the shell, indicating that $B_2 \ll B_1$, $B_3 \ll B_1$, and $B_4 \ll B_1$. Considering that the emissivity of the electron beam is much less than 1, we obtain $B_1 \ll e_{b1}$. Therefore, we can approximate (4) as follows:

$$\varepsilon_{ec}A_e e_{b1} = F_{e-h}A_eB_1 + F_{e-r}A_eB_1 + F_{e-s}A_eB_1. \tag{18}$$

Considering that $F_{e-h}+F_{e-r}+F_{e-b} = 1$, it is easy to obtain from (18) as follows:

$$B_1 = \varepsilon_{ec}e_{b1}. \tag{19}$$

According to the Stefan–Boltzmann law, we obtain

$$e_{b1} = \sigma T_e^4. \tag{20}$$

Thus, the net heat transfer from the electron beam to the SWS parts (over the length of the helix pitch) can be written as

$$Q_{e-h} = \varepsilon_{ec}A_eF_{e-h}\sigma T_e^4 \tag{21}$$
$$Q_{e-r} = \varepsilon_{ec}A_eF_{e-r}\sigma T_e^4 \tag{22}$$
$$Q_{e-s} = \varepsilon_{ec}A_eF_{e-s}\sigma T_e^4 \tag{23}$$

where Q_{e-h}, Q_{e-r}, and Q_{e-s} are the heat transfer from the electron beam to the helix, the support rods, and the tube shell, respectively. By using the parameters shown in Table I, the view factors can be calculated with (1)–(3), and are found to be $F_{e-h} = 0.545$, $F_{e-r} = 0.149$, and $F_{e-s} = 0.306$, respectively. The electron beam surface over the helix pitch A_e is calculated to be 2.903 mm^2. By using the parameters in Table I, the heat transfer from (21) to (23) can be calculated and is found to be $Q_{e-h} = 4.61 \times 10^{-5}$ W, $Q_{e-r} = 1.26 \times 10^{-5}$ W, and $Q_{e-s} = 2.59 \times 10^{-5}$ W (over the length of the helix pitch), respectively.

B. Simulation Results

To analyze the impact of thermal radiation from the electron beam on the thermal state of the operating helix TWT, we first build the structure of the helix TWT in CST Studio Suite, as shown in Fig. 4. Then, we analyze the beam–wave interaction process of the helix TWT with a PIC simulation at 11 GHz in CST Studio Suite. We obtain the electron collision loss and the ohmic loss from the PIC simulation, which are later used as the thermal source in the thermal analysis. Meanwhile, we also assign the calculated heat transfer using (21)–(23) due to thermal radiation from the electron beam to the simulation

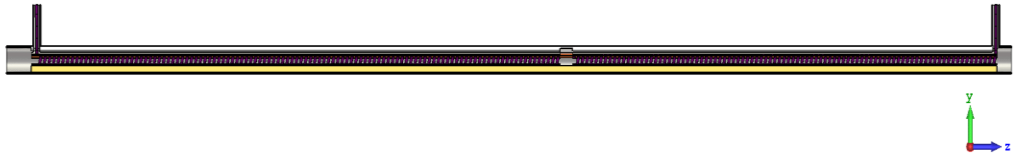

Fig. 4. Structure of the analyzed helix TWT in CST Studio Suite.

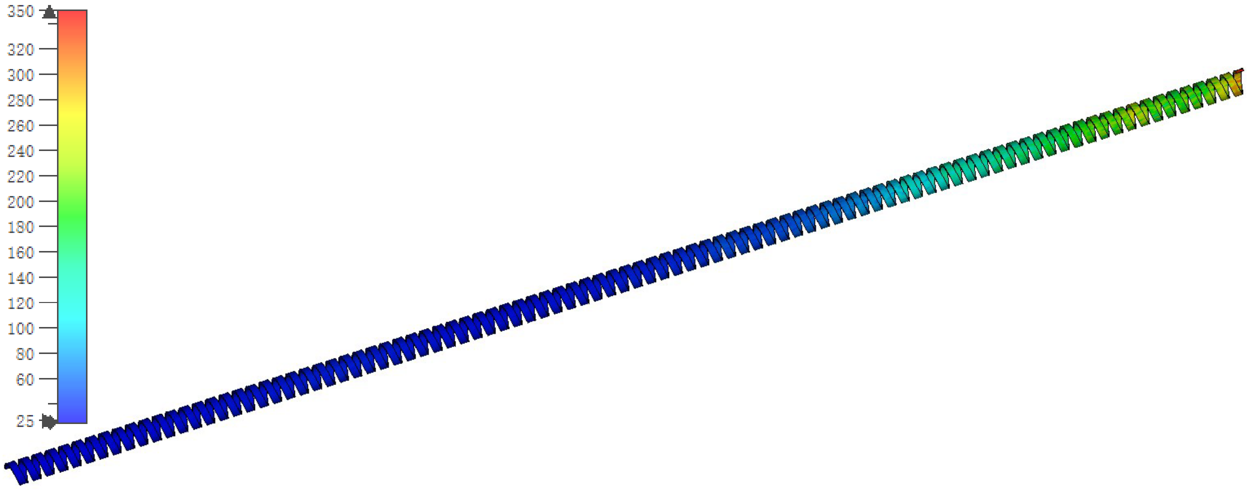

Fig. 5. Temperature distribution along the helix in the TWT.

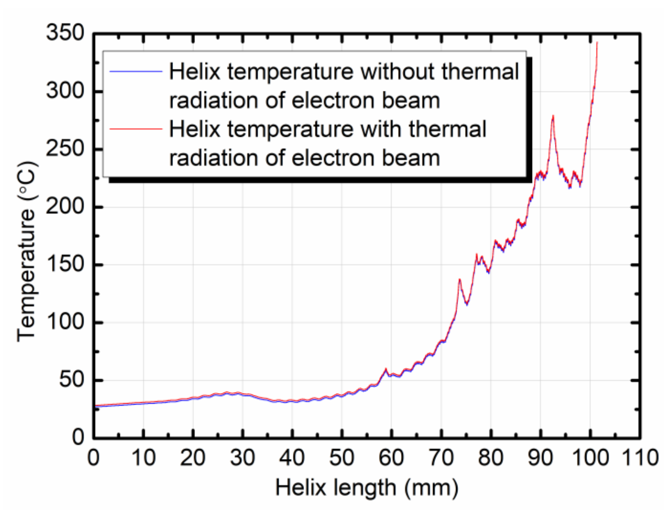

Fig. 6. Temperature distribution along the inner surface of the helix tape.

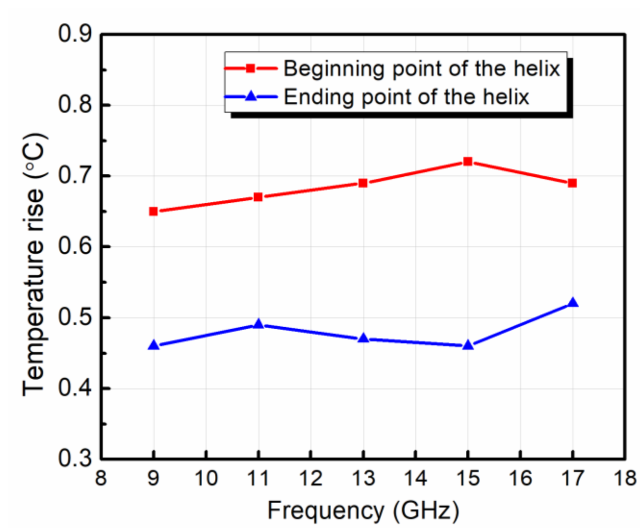

Fig. 7. Temperature increase on the inner surface of the helix tape due to thermal radiation from the electron beam in the working frequency band.

model. Then, we conduct the thermal analysis for the helix TWT. A room temperature of 20 °C is considered, and the material properties of components are also considered in the simulation. The 3-D temperature distribution is obtained, as shown in Fig. 5. It shows that the variation of the temperature on the helix (from 27.22 °C to 342.43 °C), and the high temperature concentrates on the end of the helix.

The temperature distribution along the inner surface of helix tape in the longitudinal direction is evaluated in Fig. 6, in which the results with and without considering the thermal radiation of the electron beam are compared. We can see that, in both situations, the temperature generally increases with the axial distance, and the high-temperature area is the part near the output port, which agrees with our previous work [4]. From the comparison, we see that the temperature when considering thermal radiation from the electron beam is slightly higher (0.49 °C–0.67 °C), as denoted by the red line, which is slightly above the blue line, i.e., without considering thermal radiation from the electron beam. Thus, we find that the thermal radiation from the electron beam may contribute to the temperature rise inside the helix TWT. The temperature increase due to the radiation from the electron beam reaches its maximum of 0.67 °C at the beginning point of the helix, while its minimum is 0.49 °C at the ending point connecting the output port. This is because the heat generation due to electron collision loss and ohmic loss is relatively lower in the beginning part of the helix, suggesting that the contribution of the thermal radiation from the electron beam is relatively greater. It can be concluded that the temperature increase caused by the radiation from the electron beam is not negligible, but it is also not large due to the low emissivity (4.34×10^{-10}).

We then extend our analysis on the contribution of the thermal radiation from the electron beam to the following frequencies: 9, 11, 13, 15, and 17 GHz. At each frequency, we record the temperature increase on the inner surface of the helix tape at the beginning/ending point, as shown in Fig. 7. We find that the temperature increase at the beginning point of the helix ranges from 0.65 °C to 0.72 °C in the working band, while the result at the ending point of the helix ranges from 0.46 °C to 0.52 °C. This shows that the thermal radiation from the electron beam may moderately contribute to the temperature increase inside the helix TWT in the working frequency band. The result at higher frequencies (15 and 17 GHz) is a little larger because the contribution of ohmic loss and electron collision loss is relatively small.

V. Conclusion

In this article, the thermal radiation from the electron beam in the helix TWT and its impact on the inner thermal state are explored. First, a theoretical model for analyzing heat transfer by thermal radiation from the cylindrical electron beam is proposed, in which the beam over the length of a period is equivalently treated as a circular disk. It is assumed that graybody radiation occurs only on the side surface of the disk. The view factors between the electron beam and helix/support rods/shell are calculated, and the corresponding net heat transfer is derived theoretically. Also, the heat transfer of a sheet electron beam in the chamber is derived theoretically.

Then, the thermal parameters of the electron beam are analyzed theoretically. We obtain the temperature of the electron beam using the cathode temperature and the compression ratio. The emissivity of the cylindrical/sheet electron beam is obtained by calculating the Bremsstrahlung radiation and the cyclotron radiation power from the electron beam.

Using the parameters of an actual wideband helix TWT, the emissivity of the electron beam is calculated to be 4.34×10^{-10}, meaning that it is relatively small. The heat transfer from the electron beam to the helix/support rods/shell is also calculated. The impact of thermal radiation from the electron beam on the inner thermal state of the helix TWT is analyzed by simulation. The TWT simulation model is built, and the PIC simulation is conducted to obtain the electron collision loss and the ohmic loss, which are used as thermal sources. We then conduct thermal analysis with and without considering thermal radiation from the electron beam. We find that thermal radiation from the electron beam causes a temperature rise on the inner surface of the helix tape at 11 GHz, with its maximum/minimum of 0.67 °C–0.49 °C at the beginning/ending point of the helix, respectively. It shows that the temperature rise occurs as a result of thermal radiation from the electron beam. The simulation results in the working band show that the temperature rise at the beginning point of the helix ranges from 0.65 °C to 0.72 °C, while that at the ending point ranges from 0.46 °C to 0.52 °C. We find that thermal radiation from the electron beam could contribute moderately to the temperature rise inside the TWT. The results are also informative for other VEDs, such as megawatt (MW) gyrotrons with much stronger electron beams, which could generate thermal radiation strong enough to affect the inner thermal state significantly.

References

[1] S. Yan, L. Yao, and Z. Yang, "Effect of thermal strain in helical slow-wave circuit on TWT cold-test characteristics," *IEEE Trans. Electron Devices*, vol. 55, no. 8, pp. 2278–2281, Aug. 2008, doi: 10.1109/TED.2008.926725.

[2] G. Fleury, C. Deville, and J.-C. Kuntzmann, "Average power limits of brazed-helix TWT's," in *IEDM Tech. Dig.*, Dec. 1980, pp. 806–809, doi: 10.1109/IEDM.1980.189961.

[3] P. J. Rocci, "Thermal-structural reliability assessment of helix TWT interaction circuit using finite element analysis," in *Proc. IEEE Nat. Aerosp. Electron. Conf. (NAECON)*, Jun. 1993, pp. 731–737.

[4] J. Zhang et al., "Impact of thermal state on backward-wave oscillation in helix TWT under operation," *IEEE Trans. Electron Devices*, vol. 65, no. 6, pp. 2227–2235, Jun. 2018, doi: 10.1109/TED.2017.2786029.

[5] Y. Han, Y.-W. Liu, Y.-G. Ding, P.-K. Liu, and C.-H. Lu, "Thermal analysis of a helix TWT slow-wave structure," *IEEE Trans. Electron Devices*, vol. 55, no. 5, pp. 1269–1272, May 2008, doi: 10.1109/TED.2008.919536.

[6] J. A. Lucken, "Some aspects of circuit power dissipation in high power CW helix traveling-wave tubes, part I: General theory," *IEEE Trans. Electron Devices*, vol. ED-16, no. 9, pp. 813–820, Sep. 1969, doi: 10.1109/T-ED.1969.16858.

[7] M. K. Alaria, S. Sharma, A. K. Sinha, and V. Srivastava, "Thermal analysis of slow wave structure for a space helix travelling wave tube," *Indian J. Pure Appl. Phys.*, vol. 48, no. 12, pp. 904–907, Dec. 2010.

[8] J. H. Lienhard, "Introduction," in *A Heat Transfer Textbook*, 3rd ed., Cambridge, MA, USA: Courier Corporation, 2005, pp. 3–48.

[9] G. R. Brewer, "Some characteristics of a magnetically focused electron beam," *J. Appl. Phys.*, vol. 30, no. 7, pp. 1022–1038, Jul. 1959, doi: 10.1063/1.1776975.

[10] J. R. Pierce and L. R. Walker, "'Brillouin flow' with thermal velocities," *J. Appl. Phys.*, vol. 24, no. 10, pp. 1328–1330, Oct. 1953, doi: 10.1063/1.1721158.

[11] A. S. Gilmour, "Electron beams," in *Klystrons, Traveling Wave Tubes, Magnetrons, Cross-Field Amplifiers, and Gyrotrons*. Norwood, MA, USA: Artech House, 2011, pp. 133–199.

[12] A. Warner, K. Carlson, L. Prost, and M. Sutherland, "Electron beam temperature measurements at the fermilab medium energy electron cooler," in *Proc. DIPAC*, Venice, Italy, 2022, pp. 268–270.

[13] C. Cutler and M. Hines, "Thermal velocity effects in electron guns," *Proc. IRE*, vol. 43, no. 3, pp. 307–315, 1955.

[14] P. Birtel, J. Wegener, J.-F. David, and E. Bosch, "Space-TWT beam focusing including thermal electrons," in *Proc. IEEE Int. Vac. Electron. Conf. (IVEC)*, Apr. 2016, pp. 1–2.

[15] H. Yonezawa and Y. Okazaki, "A one-dimensional disk model simulation for klystron design," Stanford Linear Accel. Center, Stanford Univ., Stanford, CA, USA, Tech. Rep. SLAC-TN-84-5, 1984.

[16] J. H. Lienhard, "Radiative heat transfer," in *A Heat Transfer Textbook*, 4th ed., Cambridge, MA, USA: Courier Corporation, 2013, pp. 525–594.

[17] I. Martinez. (2025). *Radiative View Factors*. Accessed: May 9, 2025. [Online]. Available: http://imartinez.etsiae.upm.es/

[18] L. Yao, Z. Yang, B. Li, L. Liao, B. Zeng, and X. Zhu, "Thermal analysis of novel helix TWTs," in *Proc. IEEE Int. Vac. Electron. Conf. Jointly IEEE Int. Vac. Electron Sour.*, Sep. 2006, pp. 139–140, doi: 10.1109/IVELEC.2006.1666223.

[19] A. A. Kamal, "Thermodynamics and statistical physics," in *1000 Solved Problem in Modern Physics*. Berlin, Germany: Springer, 2010, pp. 247–290.

[20] A. Piel, "Single particle motion in electric and magnetic fields," in *Plasma Physics*. Berlin, Germany: Springer, 2010, p. 50, doi: 10.1007/978-3-642-10491-6.

[21] P. M. Bellan, "Non-neutral plasmas," in *Fundamentals of Plasma Physics*. Cambridge, U.K.: Cambridge Univ. Press, 2008, pp. 460–482.

[22] B. R. Beck, J. Fajans, and J. H. Malmberg, "Temperature and anisotropic-temperature relaxation measurements in cold, pure-electron plasmas," *Phys. Plasmas*, vol. 3, no. 4, pp. 1250–1258, Apr. 1996.

[23] T. J. Birmingham, J. M. Dawson, and R. M. Kulsrud, "Contribution of electron-electron collisions to the emission of bremsstrahlung by a plasma," *Phys. Fluids*, vol. 9, no. 10, pp. 2014–2025, Oct. 1966.

[24] S. Hayakawa, Y. Terashima, T. Tsuneto, and N. Hokkyo, "Cyclotron radiation from a magnetized plasma," in *Proc. 2nd UN Int. Conf. Peaceful Uses At. Energy*, 1959, pp. 385–387.